TRANSIENT MELTING AND RE-SOLIDIFICATION OF CANDU CORE DEBRIS IN SEVERE ACCIDENTS

J.T.Rogers and M.Lamari
Dept. of Mechanical and Aerospace Engineering
Carleton University
Ottawa, Ontario

ABSTRACT

This paper describes a computer program simulating the transient behavior of CANDU core debris in the calandria following a severe accident. The program, DEBRIS.MLT, simulates debris heat-up from a quenched state to the melting point, melting of the debris, superheating of the molten debris above the melting temperature and its eventual cooling and re-solidification and the cooling of the solidified material. While the details of the debris melting process are unknown, the simplified models used in DEBRIS.MLT for the geometric changes occurring in this process provide the appropriate initial and final states for the debris. Simplified but physically reasonable heat transfer models are used in the program.

Results obtained by applying the model to a dominant-frequency late core disassembly accident sequence in a CANDU-6 show that the calandria would remain well-cooled throughout the entire transient as long as sufficient water is present in the shield-tank. This conclusion is insensitive to wide variations in the initial porosity and pore-size of the debris and to variations of the thermal properties of the molten material. Failure of the calandria resulting from the boil-off of the shield-tank water would not occur until more than 24 hours after the initiation of the accident, allowing time for operator intervention to mitigate the effects of the accident. Thus, the analysis strengthens the conclusion of earlier studies that the calandria vessel in a CANDU acts as an inherent core-catcher in a severe accident involving late core disassembly and debris melting.

NOMENCLATURE

C_{pm}	specific heat of molten material
Dt	time step
Dz_i	initial distance between nodes
Dz[nz]	distance from node nz to node nz+1
Dz_{ave}	thickness of material at a node
f_{mi}[nz]	molten fraction at a node at the beginning of a time step
f_{mo}[nz]	molten fraction at a node at the end of a time step
f_{mave}	average molten fraction of adjacent nodes
f_{maved}	average molten fraction of adjacent nodes nz and nz+1
f_{maveu}	average molten fraction of adjacent nodes nz and nz-1
H_m	latent heat of fusion of debris
K_{msd}	effective thermal conductivity of mixture of solid and molten debris at a node in downward direction
K_{msu}	effective thermal conductivity of mixture of solid and molten debris at a node in upward direction
k_B	effective thermal conductivity of the porous debris bed
k_c	thermal conductivity of corium

NU_u Nusselt number for corium in upward direction

NU_d Nusselt number for corium in downward direction

Q_d downward heat flux from a node

Q_{dh} volumetric decay heat source at a node at time t

Q_{mlt} total heat source per unit area for melting at a node at time t, W/m^2

Q_{sol} total heat source per unit area for solidification at a node at time t, W/m^2

Q_u upward heat flux from a node

Q_{zr} volumetric heat source from Zr + steam reaction at a node at time t

T[nz] temperature at node nz

T_i[nz] temperature at beginning of time step at node nz

T_o[nz] temperature at end of time step at node nz

t time

VOID[nz]porosity at node nz

$VOID_i$ initial uniform porosity in debris bed

ρ density of solid debris

ρ_m density of molten material

1.0 INTRODUCTION

In accident sequences in a CANDU reactor in which the fuel heat is not removed by normal or emergency coolant in the primary heat transport system (PHTS), the separately cooled moderator provides an effective heat sink which ensures that no gross melting of the fuel occurs and pressure-tube integrity is maintained (Sanderson et al (1996)).

There is a low probability that the moderator heat sink could be ineffective in these types of accidents (Howieson et al (1988), Allen et al (1990), Dick et al (1990), Blahnik et al (1993)). These studies, based on earlier work by Rogers (1984), have indicated that, although core disassembly would occur as the moderator boiled off, the core debris, whether solid or molten, would be contained within the calandria as long as it remained cooled by the shield-tank water. Boil-off of shield-tank water could eventually lead to calandria vessel failure, typically at times greater than 24 hours after initiation of the accident, allowing considerable time for operator intervention.

Recently, Meneley et al (1996) and Rogers et al (1996), have developed the improved computer codes DEBRIS.2 and MOLPOOL for analyzing such an accident. DEBRIS.2 models the transient heat-up of a bed of solid core debris in the bottom of the calandria from a quenched state to the beginning of melting within the bed. MOLPOOL models the steady-state behavior of a molten pool of core debris (corium) bounded on the top and bottom by solid crusts. At the times that a molten pool would be expected to form, the heat source would be decaying slowly enough that quasi-steady-state conditions would exist so that the steady state model should represent the pool behavior quite well. Results obtained with these improved models for a dominant-frequency late-core-disassembly (LCD) accident in a CANDU-6 reactor confirmed and strengthened the results of the earlier studies that core debris, whether solid or molten, would be retained in the calandria as long as it remained well cooled by the shield-tank water. That is, the calandria would act as an inherent "core-catcher" in such severe accidents.

At the time of the work of Meneley et al (1996) and Rogers et al (1996), no model was available to analyze the transient melting behavior of the debris with resulting changes in debris-bed geometry, i.e., there was no analytical bridge between the transient heating of the solid debris and the quasi-steady-state behavior of the molten pool. Also, no experimental data on debris-bed melting were available. To overcome these difficulties, it was assumed in those studies that the molten pool was formed instantaneously as melting began in the debris. While this is obviously a gross simplification, it was believed that the results would be conservative since the molten pool would be assumed to exist much earlier than could occur in reality.

Nevertheless, there was an obvious need for a transient model of core debris melting and eventual solidification to complete the argument that inherent processes would result in molten debris containment in the calandria as long as it is cooled by the shield-tank water. In response to this need, an analytical model, DEBRIS.MLT, has been developed under contract to AECL to describe quantitatively the behavior of the debris and the calandria wall under these conditions. The development of the model and results obtained by its application to the representative LCD accident in a CANDU-6 described by Dick et al (1990) and used by Meneley et al (1996) and Rogers et al (1996) are described in this paper. Further information is provided by Rogers (1997).

2.0 BASIS FOR THE DEVELOPMENT OF THE DEBRIS.MLT MODEL

2.1 Core Debris Heat-Up Model. DEBRIS.2

DEBRIS.MLT has been developed as an extension of the transient model describing the heat-up of solid core debris in a CANDU calandria, DEBRIS.2. DEBRIS.2 is a transient, one-dimensional, explicit finite-difference model in which the core debris in the bottom of the calandria is represented by a uniform porous bed of the core materials with porosity and average pore size specified as inputs and with distributed heat sources from decay heat and, as an option, from the zirconium-steam reaction. The model accounts for all identified heat transfer mechanisms within the bed and from the bed to the shield-tank water and for material property variations with temperature. See Figure 1. The model provides two options for the shield-tank water cooling system, operating and non-operating. A detailed description of DEBRIS.2 is given by Meneley at al (1996).

Recently, a re-assessment of the model of the effective thermal conductivity of the porous solid debris bed, based on the work of Hsu et al (1995), resulted in the development of an improved model (Rogers, 1997). The improved model for the effective thermal conductivity of the porous bed is incorporated in the DEBRIS.MLT program.

2.2 Molten Pool Model. MOLPOOL

DEBRIS.MLT also adapts certain elements of the molten pool model MOLPOOL. MOLPOOL models the behavior of molten core debris (corium) in a CANDU calandria. MOLPOOL consists of a steady-state, lumped-parameter model of a molten pool bounded by upper and lower solid crusts. The pool is assumed to be homogeneous with no stratification of the various materials occurring. The model allows for decay-heat generation in the molten pool and in the solid crusts and predicts the thicknesses of the crusts. It accounts for internal natural convection and radiation heat transfer to the upper and lower surfaces of the pool using correlations from the literature as well as heat transfer by all identified mechanisms from the surfaces of the pool to the shield-tank water. See Figure 1. For further information, see Meneley et al (1996).

3.0 THE DEBRIS.MLT MODEL

As noted above, the DEBRIS.MLT model has been developed as an extension of the DEBRIS.2 model, incorporating certain modified elements of the MOLPOOL model as well as the improved model for the debris-bed thermal conductivity discussed in section 2.1. The extension of the DEBRIS.2 model consists mainly of modifications to the existing sub-routine FDR. This sub-routine solves the basic finite-difference equations for the transient thermal behavior of the porous solid debris bed resulting from the core disassembly. DEBRIS.MLT also includes a new sub-routine, MLTPLHT, which incorporates correlations adapted from MOLPOOL to describe natural convection and internal radiation heat transfer in a volume-heated molten pool.

The processes that are modelled in the modified sub-routine FDR, in addition to the initial heating of the porous solid debris bed as described in section 2.1, consist of melting of the debris at a constant temperature once a node has reached the melting temperature, superheating above the melting temperature of the molten material after all the debris in a node has melted, eventual cooling of the corium as the heat source decays, re-solidification at a constant temperature of corium in a node because of continuing heat source decay, and cooling of re-solidified material in a node. Accompanying the melting of material in a node are geometry changes which are also modelled.

3.1 The Melting Process

In a mixture of materials with different melting points as in the core debris, melting will begin first for the material with the lowest melting temperature. As the temperature rises above this point other materials will begin to melt or to dissolve in already molten material. Thus, complete melting of the mixture will occur over a range of temperatures. However, to simplify the model it is assumed, as noted above, that melting of the debris occurs at a constant temperature which is an input to the computer program. Thus, once the melting temperature at a node has been reached, the temperature at the node remains constant until all the material at that node has melted. The fraction of molten material in a node at the end of a given time step is calculated by a heat balance on the node, assuming a constant value of the latent heat of fusion, H_m:

$$f_{mo}[nz] = (Q_{mlt} * Dt) / (\rho * Dz_{ave} * H_m) + f_{mi}[nz] \qquad (1)$$

where $f_{mi}[nz]$ is the molten fraction in the node at the beginning of the time step and Q_{mlt} is the net heat source per unit area in the node at time t, allowing for decay heat and any heat generated by the zirconium-steam reaction as well as heat losses from the node. Q_{mlt} is given by:

$$Q_{mlt} = (Q_{dh} + Q_{zr})*Dz_{ave} - Q_u - Q_d \qquad (2)$$

In equation 2, Q_{dh} is the effective volumetric decay heat source at a node, making appropriate allowance for the dilution effect of the ZrO_2 and the presence of porosity in the bed (Rogers (1997)). Q_{zr} is the volumetric heat source from the zirconium-steam reaction at the node (Meneley et al (1996)) and Q_u and Q_d are the upward and downward heat fluxes, respectively, from the node in question to the adjacent nodes, given by:

$$Q_u = K_{msu} * (T[nz] - T[nz-1]) / Dz[nz-1] \qquad (3)$$

$$Q_d = K_{msd} * (T[nz] - T[nz+1]) / Dz[nz] \qquad (4)$$

where:

$$K_{msu} = k_B * (1-f_{maveu}) + k_c * NU_u * f_{maveu} \qquad (5)$$

$$K_{msd} = K_B * (1-f_{maved}) + k_c * NU_d * f_{maved} \qquad (6)$$

K_{msu} and K_{msd} are the effective thermal conductivities of a mixture of solid and molten debris in the upward and downward directions respectively. These are calculated as the weighted sum of the effective thermal conductivities of the porous solid debris and of the molten corium for the adjacent nodes in question. The effective thermal conductivity for the porous solid debris is determined as described in section 2.1. The effective thermal conductivity of the molten corium allows for natural convection of the corium by multiplying its actual thermal conductivity by an appropriate Nusselt number for corium natural convection for the node conditions and for heat flow in the appropriate direction. The weighting is based on the average solid and molten fractions of the adjacent nodes.

The appropriate Nusselt numbers for corium natural convection are calculated in the new sub-routine MLTPLHT using correlations from the literature for natural convection in a volume-heated molten pool to flat upper and lower surfaces. For the upper surface, the correlation of Kulacki and Goldstein (1972) is used, as in MOLPOOL. For the lower surface, the correlation of Jahn and Reineke (1975), as reported by Steinberner and Reineke (1978) and Gabor et al (1979), is used. At the high temperatures of molten corium, internal thermal radiation heat transfer must be accounted for (Stein et al (1979)). Therefore, for heat transfer to both upper and lower surfaces, the Nusselt numbers are modified to account for the effects of internal thermal radiation on thermal conductivity, using the approach of Anderson (1976). Reference property values used for the molten corium are those of Park et al (1994). Data from Anderson (1976), Rempe et al (1992) and Abalin et al (1996) were used to establish sensitivities.

The form of equations 5 and 6 implies that the mechanisms of heat transfer through the porous solid material and through the molten material act in parallel. This may appear to be an over-simplified model. However, since the temperature of a node remains constant at the melting temperature throughout the melting process, the precise value of the effective heat transfer coefficient between partially molten nodes is not important since no heat transfer between them can occur in any case. For the case of a solid-debris node adjacent to a partially molten node, the exact mode of heat transfer in the partially molten node is again not very important since heat transfer to or from that mode occurs in series with that of the solid-debris node, which represents the governing mechanism. Equations 5 and 6 reduce to the correct values for the heat transfer rates between nodes at the limiting cases of no melting ($f_{mave}=0$) and of complete melting ($f_{mave}=1$).

In equations 3 and 4 the distance betwen nodes, Dz[nz], is treated as a variable that may change with node position and time. This treatment allows for changes in debris geometry after melting begins. As melting progresses, molten corium will fill the voids in the debris bed and the melting of debris will also cause re-arrangement (collapse) of remaining solid material. While the details of these processes are not known, the end-states of the distance between nodes are known: initially a distance, Dz_i, calculated from the maximum height of the bed (determined by the quantities and densities of materials present, the geometry of the calandria and the assumed porosity of the bed) and the number of nodes used and finally, for complete melting, a distance corresponding to zero porosity corrected by any change in densities of the materials during the melting process. Therefore, a simple model for the geometry change during melting is assumed in which the porosity at a node and the distance between nodes are functions of the molten fraction at the node, as follows:

$$\mathrm{VOID}[nz] = \mathrm{VOID}_i * (1 - f_{mo}[nz]) \qquad (7)$$

$$Dz[nz] = Dz_i * (1-\mathrm{VOID}_i) / (1-\mathrm{VOID}[nz]) \qquad (8)$$

In equation 8, no allowance for change in material densities during the melting process has been made since it has been shown to have an insignificant effect on molten pool behavior in the earlier study (Meneley et al (1996)).

This model of the melting process implies that molten material does not move from a given node to lower one under the influence of gravity but remains within its original node during the melting process. Considering the high viscosity of the molten material at its melting point and the complexity of the porous debris bed structure, this model may at least approximate the actual melting process behavior. In any case as we will see, the model does result in an end state for the debris that represents the expected end-state reasonably well, i.e., a "collapsed" bed consisting of a molten pool with top and bottom "crusts" and a total thickness close to the expected value.

3.2 Superheating and Eventual Cooling of Corium

Once all the material in a node is molten, the temperature of the node begins to rise again, assuming the heat generation rate at this time is greater than the net heat loss rate from the node. The heat balance equation for the node reverts to the form used for the heat-up of the solid debris, as in DEBRIS.2:

$$T_o[nz] = \{[(Q_{dh}+Q_{zr})*Dz_{ave}-Q_u-Q_d]*Dt\}/(C_{pm}*\rho_m*Dz_{ave}) + T_i[nz] \qquad (9)$$

The physical properties in equation 9 are now those for molten corium and the equations for heat losses and gains, Q_u and Q_d, are now given by equations 3 to 6 with $f_{mave} = 1.0$, using equations 7 and 8 with VOID[nz] = 0 and Dz[nz] = $Dz_i * (1 - VOID_i)$.

For superheated corium conditions, the model thus treats a node as a cell with heat transfer to or from the adjacent nodes (cells) by natural convection to or from upper and lower flat surfaces, depending on the direction of the heat flow. The direction of heat flow is determined by the temperature differences between the node in question and the adjacent nodes at the beginning of the time-step. While this model does not closely represent a relatively deep molten pool in which the natural circulation would occur between the top and bottom of the pool, the additional thermal resistances represented by the cells would not affect temperatures and surface heat fluxes greatly because of the very high heat transfer rates occurring between the cells with natural convection of the molten material. In any case, the predicted maximum pool temperature will be conservative.

The model assumes that the molten corium remains homogeneous, that is that no stratification of the different materials occurs, such as metallic melt separation from the oxidic corium pool.

As the decay heat source decreases with time and all the zirconium is consumed in the reaction with steam, the node temperatures predicted by equation 9 will eventually reach maximum values and begin to decrease under the continuing influence of the heat losses from the nodes.

3.3 Re-solidification of Corium and Eventual Cooling of Re-solidified Debris

As the corium at a node cools, its temperature eventually reaches a value at which the corium begins to re-solidify. In this study, this solidification temperature is assumed to be the same as the melting temperature of the solid debris[1]. This temperature is assumed to be constant during the solidification process, i.e., the temperature range corresponding to the difference between the liquidus and solidus temperatures is ignored. For the expected composition of the solidifying corium this range is quite small (MATPRO (1990)). Also, any separation of materials during the solidification process is ignored in this analysis.

As in the case of melting, once the solidification temperature at a node has been reached, the temperature at the node remains constant as the heat of fusion is released until all the material at that node has solidified. Again as for melting, the fraction of molten material at a node at the end of a given time step is calculated by a heat balance on the node, assuming the same constant value of the latent heat of fusion as used in the melting process:

$$f_{mo}[nz] = (Q_{sol} * Dt) / (\rho * Dz_{ave} * H_m) + f_{mi}[nz] \qquad (10)$$

where $f_{mi}[nz]$ is the molten fraction in the node at the beginning of the time step and Q_{sol} is the (negative) heat source per unit area at time t, allowing for decay heat and the net heat losses from the node. It is assumed that there is no longer any heat being generated by the zirconium-steam reaction. Therefore, Q_{sol} is given by:

---

[1] In reality, the solidification temperature will be somewhat lower than the melting temperature since the liquidus temperature of the UO_2 - ZrO_2 system corresponding to the expected mole fraction of ZrO_2 in the corium for a CANDU-6 core will be in the range of 2550°C to 2600°C compared to the melting temperature of pure ZrO_2 of about 2700°C and pure UO_2 of about 2850°C (MATPRO (1990))

$$Q_{sol} = Q_{dh}*Dz_{ave} - Q_u - Q_d \qquad (11)$$

As before, Q_u and Q_d are the upward and downward heat fluxes, respectively, from the node in question to the adjacent nodes, given by equations 3 to 6, using equations 7 and 8 with VOID[nz]=0 and $Dz[nz]=Dz_i*(1-VOID_i)$, since there is now no void in the solidified material. This means that the distances between re-solidifying nodes remain constant, since the effect of the change in density as the material solidifies is ignored, as noted earlier. Also, because of the absence of void, the value of k_B for the solid material includes only the effect of solid conduction since radiation and steam conduction across voidage pores are now non-existent.

Once all the material at a node is solidified, i.e., when $f_{mo}[nz] = 0$, the node temperature begins to fall under the combined effect of the decay heat source and the dominating heat losses to the adjacent nodes. The heat balance equation at the node reverts to that used for the initial heat-up of solid material with the heat loss rates given by Q_u and Q_d with VOID[nz]=0 and $Dz[nz]=Dz_i*(1-VOID_i)$ as described in the previous paragraph.

4.0 RESULTS

4.1 Reference Conditions

The reference conditions for the study are essentially those used by Meneley et al (1996) and Rogers et al (1996) for a dominant-frequency LCD accident in a CANDU-6 reactor. The earlier studies have shown that in such an accident a quenched debris bed composed of coarse, solidified material located in the bottom of the calandria would begin to heat up about five hours after the initiating event. For the reference case, it is assumed that the debris melting and solidification temperatures are 2700°C, all of the zirconium in the core has already been oxidized to ZrO_2 before the heat-up begins, all of the debris falls into the main calandria shell and the shield tank cooling system is not operational. Other input data and information used for the reference case are given by Rogers (1997).

The reference values for the initial debris-bed porosity, 0.5, and average pore size, 3 cm, are the same as used earlier. As explained by Meneley et al (1996) and Rogers et al (1996), these values are based on judgements of the expected nature of the coarse debris resulting from the disassembly processes of a CANDU core in the selected accident sequence. See Blahnik et al (1993).

To ensure adequate convergence and to avoid oscillations of the results, 40 nodes and time steps of 10 seconds were used in the calculations.

4.2 Results for the Reference Case

4.2.1 Debris and Corium Temperatures

Figure 2 shows the temperature histories at different points in the debris and corium for the reference conditions. Temperatures shown are the maximum temperature, the top temperature and the bottom temperature. The solid debris heats up until the melting point at the hottest node is reached at about 415 minutes. The maximum temperature, which occurs at a node at about the mid-point of the debris, remains at the melting point, 2700°C, until all the debris at this node has melted. This occurs at about 475 minutes, so that complete melting at this node takes about 60 minutes. Superheating of the corium at this node then begins with the temperature of the molten corium reaching a maximum of about 3060°C at about 540 minutes[2]. From this time on, the maximum temperature drops slowly to about 2950°C at 1200 minutes so that the debris at this node is still molten at this time.

Figure 2 shows that the top and bottom temperatures of the debris and corium remain well below the debris

---

[2] This maximum temperature is well below the boiling-point temperature range expected for typical UO_2–ZrO_2 corium mixtures of about 3250°C to 3450° (Anderson (1976)), so that no boiling in the molten pool would be expected.

melting temperature throughout the melting transient, extending a major conclusion of the earlier studies, that molten debris is bounded top and bottom by solid material or crusts, to the period of the debris-melting transient.

Figure 2 also shows the temperatures predicted for the same conditions by the quasi-steady-state model MOLPOOL. Considering the differences between the two models, particularly the nature of the crusts, porous structures in DEBRIS.MLT and a solid homogeneous mixture in MOLPOOL, reasonable agreement is obtained between the temperatures of the debris predicted by the two programs at all times beyond 600 minutes when the quasi-steady-state assumption used in MOLPOOL would be expected to be valid.

Figure 3 shows temperature profiles through the debris and corium at different times for the reference conditions. At 350 minutes, some time before melting begins at about 415 minutes, the temperature profile is very flat, at a value of about 1350°C, over a large central region of the debris bed. The temperature in this region is rising under approximately adiabatic conditions, with the heat generation rate dominating the heat loss rate. At 450 minutes, about 35 minutes after melting begins, the central region is at the melting temperature, 2700°C, with the temperature dropping rapidly above node 5, about 16 cm from the top surface, and below node 35, about 20 cm from the bottom surface. A profile is also shown for the time, 540 minutes, at which the molten corium reaches its maximum temperature, 3060°C. The central region still occupies the same nodes as before, but it has been reduced in size, as we will see, because the node sizes have decreased as melting proceeds. At 1200 minutes, the corium temperatures have decreased but the molten corium region stil occupies the same nodes.

4.2.2 Molten Fractions and Debris Depth

Figure 4 shows the molten fractions at different positions as functions of time for the reference conditions. Nodes 1 to 4 undergo no melting at any time during the transient. Node 5 is the first node from the top to undergo melting, beginning at about 460 minutes, with its molten fraction reaching a peak of about 0.98 at about 530 minutes and decreasing steadily thereafter. Node 6 begins melting at about 425 minutes, very soon after melting first begins in the debris, and its molten fraction increases steadily thereafter, reaching complete melting at about 500 minutes. Node 6 then remains completely molten over the rest of the period to 1200 minutes. Similarly, all the nodes from 7 to 34 begin melting at about the time that melting initiates in the debris, their molten fractions increase steadily to unity over about 70 minutes and they remain completely molten to 1200 minutes. Node 35 is the closest node to the bottom to undergo partial melting, behaving in a manner very similar to that of node 5. Nodes 36 to 40 undergo no melting at any time during the transient.

The variation with time of the total depth of the debris bed during bed heat-up, melting transient and corium pool development is shown in Figure 5. After melting starts at about 415 minutes, the total height begins to decrease from the initial 1.65 metres as molten material starts to fill the voids and the node sizes begin to decrease as described in section 3.1. The total depth, including top and bottom "crusts" and the molten pool, reaches a minimum of about 1.0 metres at about 520 minutes and remains constant after that time.

4.2.3 Heat Fluxes to Shield-Tank Water and Calandria Wall Temperatures

Figure 6 shows some of the most important results, the heat fluxes to the shield-tank water from the calandria wall. The heat flux from the wall below the debris reaches a peak of about 11.5 W/cm^2 at about 480 minutes and decreases steadily after that time. The heat flux from the wall above the debris reaches a peak of about 9.3 W/cm^2 at about the same time, decreasing thereafter. It is important to know how these heat fluxes compare to the critical heat flux (CHF) for these conditions. Experimental results relevant to the present case are those of Cheung and Haddad (1994), Haddad et al (1995) and El Genk and Glebov (1995) for CHF on downward-facing hemispherical surfaces. For saturated water at atmospheric pressure, the minimum quasi-steady-state CHF observed in these studies was about 50 W/cm^2 to 62 W/cm^2 at the bottom of the hemisphere. For the shield tank pressure at the bottom of the calandria, CHF would be higher. These values are well above the maximum predicted downward heat flux of about 11.5 W/cm^2 for the reference case. Therefore, we can conclude that CHF will not occur under the reference conditions during the melting transient.

The stainless steel calandria wall temperatures as a function of time for the reference conditions are shown in Figure 7. The average wall temperature, i.e., the average of the inside and outside surface temperatures is always less than about 250°C for both the top and bottom surfaces, well below the level at which creep rupture would be a concern. Considering this and the finding that CHF will not occur on the calandria wall, we can conclude for the reference conditions that the calandria wall will remain well-cooled throughout the transient and that the integrity of the calandria will be maintained. Failure of the calandria resulting from the boil-off of shield-task water would not occur until more than 24 hours after the start of the accident (Meneley et al (1996), Rogers et al (1996)).

4.3 Results of Sensitivity Studies

4.3.1 Effects of Initial Debris-Bed Porosity

The effects of the variation of the initial debris-bed porosity from 0.1 to 0.85 on key debris temperatures are shown in Figure 8, for the reference pore size of 3 cm. There is essentially no effect of porosity on the maximum bed temperature up to the moment that melting begins, in agreement with the results obtained using DEBRIS.2 (Meneley et al (1996), Rogers et al (1996)). In each case, of course, the temperatures during the melting transient are constant at 2700°C. Complete melting at this node occurs at about the same time, 475 minutes, for the entire range of porosities, as would be expected since the same mass of material must be melted, under essentially adibatic conditions, irrespective of the porosity. The peak corium temperature reached is higher for a porosity of 0.1, about 3150°C, than for the reference porosity of 0.5, about 3060°C, and for a porosity of 0.85, about 2950°C.

Figure 8 shows that the top and bottom temperatures of the debris are not affected greatly by initial debris-bed porosity. Both top and bottom temperatures are well below the melting temperature throughout the transient, whatever the bed porosity. In addition, there are only small differences in the calandria wall heat fluxes to the shield-tank water during the transient over the porosity range of 0.1 to 0.85, for the reference average pore size of 3 cm. In particular, the peak heat flux is always below 12 W/cm^2 so that CHF would not occur.

Finally, variation of the debris porosity over the range 0.1 to 0.85, for the reference pore size of 3 cm, resulted in only minor differences in calandria wall temperatures during the transisent.

4.3.2 Effects of Initial Debris-Bed Pore Size

An assessment was also made of the effect of the variation of average pore size from 1 cm to 11 cm on the transient thermal behavior of the debris for the reference porosity of 0.5, as in the earlier study (Meneley et al (1996), Rogers et al (1996)). This variation had only slight effects on the maximum temperature and the top and bottom temperatures of the debris. There is practically no change in calandria-wall heat fluxes to the shield tank water or calandria wall temperatures as the pore size varies over the range examined. Thus, predicted debris thermal behavior throughout the transient is quite insensitive to initial average pore size for the reference case porosity.

4.3.3 Effects of Corium Property Values

Variation of the thermal conductivity of the molten corium over a range from 2 W/mK to 10 W/mK compared to the reference value of 3.6 W/mK had only minor effects on the maximum corium temperature, with the temperature being reduced slightly as corium thermal conductivity was increased, as would be expected. There were essentially no effects on any other parameters.

Variation of the corium absolute viscosity from the reference value of 0.00328 kg/m s to a value of 0.0068 kg/m s (Abalin et al (1996)) resulted in negligible effects on all key parameters.

5.0 ASSESSMENT AND CONCLUSIONS

This paper has described the development of an integrated analytical model of transient debris heat-up, melting, corium superheating and cooling and solidification and solid cooling to simulate the thermal behavior of CANDU core debris in the calandria in an LCD accident. Results obtained by applying this model to the dominant-frequency CANDU-6 accident sequence considered in the previous study (Meneley et al (1996) and Rogers et al (1996)) have filled in a gap in that study, the period of transient melting and corium superheating and cooling. These results confirm and strengthen the conclusions of the previous study that the calandria walls would remain well-cooled by the shield-tank water in the event of an LCD accident in a CANDU-6 and that the calandria would contain the debris, whether molten or solid, and maintain its integrity until its uncovery. Adequate time would be provided for operator intervention before calandria uncovery and failure could occur due to shield-tank water boil-off. The present results confirm once more that the calandria would act as an inherent core-catcher in such an accident as long as the shield-tank water is present.

As before, this conclusion is reasonably insensitive to channel-failure mechanism, core-collapse mechanism, debris porosity and pore size. It is believed to be insensitive also to the mechanism of debris melting and the accompanying geometry changes. The conclusion is also insensitive to variations in corium thermal conductivity and absolute viscosity.

Some questions and uncertainties remain, such as:

* the mechanical/thermal behavior of the end-shields
* the capacity of the shield-tank relief system
* local hot-spot effects in the debris
* local obstructions to natural circulation flow of the shield-tank water
* the adequacy of the debris melting model
* debris and corium property values

An experimental program on simulated core disassembly now in progress at AECL will produce information that should reduce the uncertainties in the analysis, by confirming the initial state of the quenched debris. The co-operative international RASPLAV program, in which AECL is participating, will provide information on the behavior of corium in accidents and on corium property values that will help to reduce uncertainties. A review of the calandria design should identify and eliminate, if possible, local regions of potential recirculation flow interference and vapor trapping on the calandria surface in the shield tank. If it is not possible to eliminate such regions, analysis on a local basis would be needed, backed up by small-scale experiments if necessary, to demonstrate adequate cooling. The effects on the end-shields of an LCD accident sequence should also be investigated. Finally, the likelihood and mechanism of failure of the calandria vessel as it is uncovered by the boil-off of the shield-tank water should be investigated.

Nevertheless, the results of the analysis described in this paper provide further confidence that the calandria vessel in a CANDU-6 reactor would act as an inherent core-catcher in an LCD accident and that adequate time would be provided for operator intervention to mitigate the effects of the accident.

REFERENCES

Abalin, S.S., V.G.Asmolov, V.D.Daragan, E.K.D'yakov, A.V.Merzlyakov and V.Yu.Vishnevsky (1996), Kinematic Viscosity Measurement of C-100 and C-22 Corium, OECD RASPLAV Project, RP-TR-18, April, 1996

Allen,P.J., J.Q.Howieson, H.S.Shapiro, J.T. Rogers, P.Mostert and R.W. van Otterloo (1990), Summary of CANDU 6 Probabilistic Safety Assessment Study Results, Nuclear Safety, Vol.31, No.2, pp.202-214

Anderson,E.A., (1976), Radiative Heat Transfer in Molten UO_2 Based on the Rosseland Diffusion Method, Nuclear Technology, Vol.30, p.65

Blahnik,C., J.C.Luxat and S.Nijhawan (1993), CANDU Response to Loss of All Heat Sinks, Proc. Ninth ANS Meeting on Nuclear Thermalhydraulics, San Francisco

Cheung,F.B., and K.H.Haddad (1994), Steady-State Observations of Critical Heat Flux Phenomena on a Downward Facing Hemispherical Surface, Proc. 23rd Water Reactor Safety Meeting, Vol.2, pp.87-112, 1994

Cheung,F.B., and K.H.Haddad (1997), A Hydrodynamic Critical Heat Flux Model for Saturated Pool Boiling on a Downward Facing Curved Heating Surface, Int.J.Heat Mass Transfer, Vol.40,No.6, pp.1292-1302, April, 1997

Dick,J.E., V.I.Nath, E.Kohn, T.K.Min and S.Prawirosoehardjo (1990), Event Sequence of a Severe Accident in a Single Unit CANDU, Nuclear Technology, Vol.90, No.5, pp. 155-167

El Genk,M.S., and A.G.Glebov (1995), Transient Pool Boiling from Downward-Facing Curved Surfaces, Int.J.Heat Mass Transfer, Vol.38, No.12, pp.2209-2224, August, 1995

Gabor,J.D., L.Baker,Jr.,J.C.Cassulo, D.J.Erskine and J.D.Warner (1979), Heat Transfer to Curved Surfaces from Heat Generating Pools, ASME Paper 79-HT-113, 18th US National Heat Transfer Conference, August 1979

Haddad,K.H., Y.C.Liu and F.B.Cheung (1995), Spatial Variation of Critical Heat Flux on a Downward Facing Hemispherical Surface, Proc. 30th National Heat Transfer Conference, ASME HTD-316, pp.22-33, 1995

Howieson,J.Q., H.S.Shapiro, P.J.Allen, J.T.Rogers, P.Mostert and R.W. van Otterloo (1988), Probabilistic Risk Assessment Study of a CANDU 600, Proc. IAEA Symposium on Severe Accidents in Nuclear Power Plants, Vol.1, pp.245-262

Hsu,C.T., P.Cheng and K.W.Wong (1995), A Lumped-Parameter Model for Stagnant Thermal Conductivity of Spatially Periodic Porous Media, J. Heat Transfer, Vol.117, No.2, pp.264-269, May, 1995

Jahn,M. (1975), PhD Thesis, University of Hannover

Kulacki,F.A., and R.J.Goldstein (1972), Thermal Convection in a Horizontal Fluid Layer with Uniform Volumetric Energy Sources, J. Fluid Mechanics, Vol.53, pp.271-287

MATPRO - A Library of Materials Properties for Light Water Reactor Accident Analysis (1990), NUREG/CR-52.3, EGG-2555, Vol.4

Meneley,D.A., C.Blahnik, J.T.Rogers, V.G.Snell and S.Nijhawan (1996), Coolability of Severely Degraded CANDU Cores, AECL-11110, July, 1995, Revised January, 1996.

Park,H., V.K.Dhir and W.E.Kastenberg (1994), Effect of External Cooling on the Thermal Behavior of a Boiling Water Reactor Vessel Lower Head, Nucl. Technology, Vol.108, pp.266-282, November, 1994

RASPLAV (1996), Pretest Analysis of Final RASPLAV-AW-200 Design, Volume 1, Main Research and Development Results, RP-TR-21, Vol.1, May, 1996

Rempe,J.L., et al (1992), Light Water Reactor Lower Head Failure Analysis, NUREG/CR-5642, March, 1992

Rogers,J.T. (1984), Thermal and Hydraulic Behavior of CANDU Cores Under Sever accident Conditions - Final Report. Vol. 1 & 2. Atomic Energy Control Board INFO-0136, June 1984

Rogers,J.T., D.A.Meneley, C.Blahnik, V.G.Snell and S.Nijhawan (1996), Coolability of Severely Degraded CANDU Cores, pp. 317-334, in Heat and Mass Transfer in Severe Nuclear Reactor Accidents, J.T.Rogers, Editor, Begell House Inc., New York

Rogers,J.T. (1997), Transient Melting and Re-Solidification Model of CANDU Core Debris in the Calandria in Severe Accidents, Report to AECL, March, 1997, Revised, August, 1997

Sanderson, D.B., R.G.Moyer and R.Dutton (1996), Effectiveness of the Moderator as a Heat Sink During a Loss-of-Coolant Accident in a CANDU-PHWR Reactor, pp. 301-316 in Heat and Mass Transfer in Severe Nuclear Reactor Accidents, J.T.Rogers, Editor, Begell House Inc., New York

Stein,R.P., L.Baker, Jr., W.H.Gunther and C.Cook (1979), Heat Transfer from Heat Generating Molten UO_2: Interpretations of the Available Experimental Data, ASME Paper 79-HT-115

Steinberner,U., and H.H.Reineke (1978), Turbulent Buoyancy Heat Transfer with Internal Heat Sources, Proc. Sixth International Heat Transfer Conference, J.T.Rogers, Editor, Toronto, Vol.2, pp.305-310

ACKNOWLEDGEMENTS

The work described in this paper was undertaken under contract to AECL. The authors thank AECL for permission to present this paper. They also thank Christie Egbert for secretarial assistance with the paper.

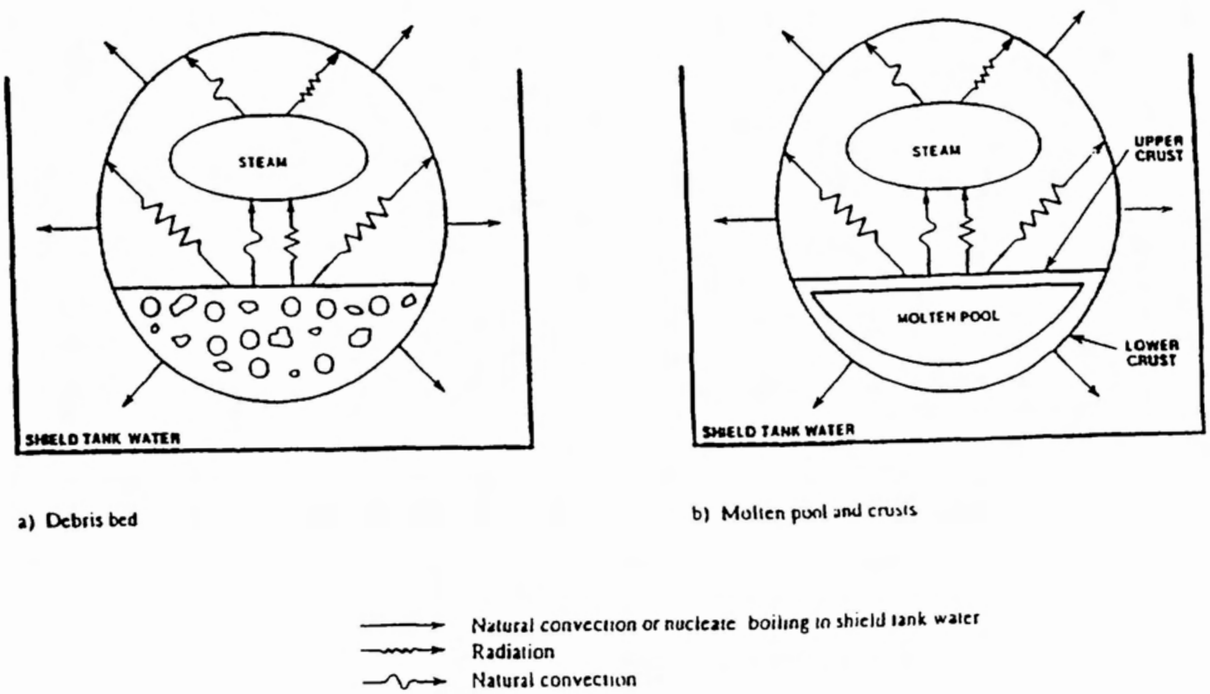

Figure 1: Analytical Model of Debris Bed and Molten Pool.

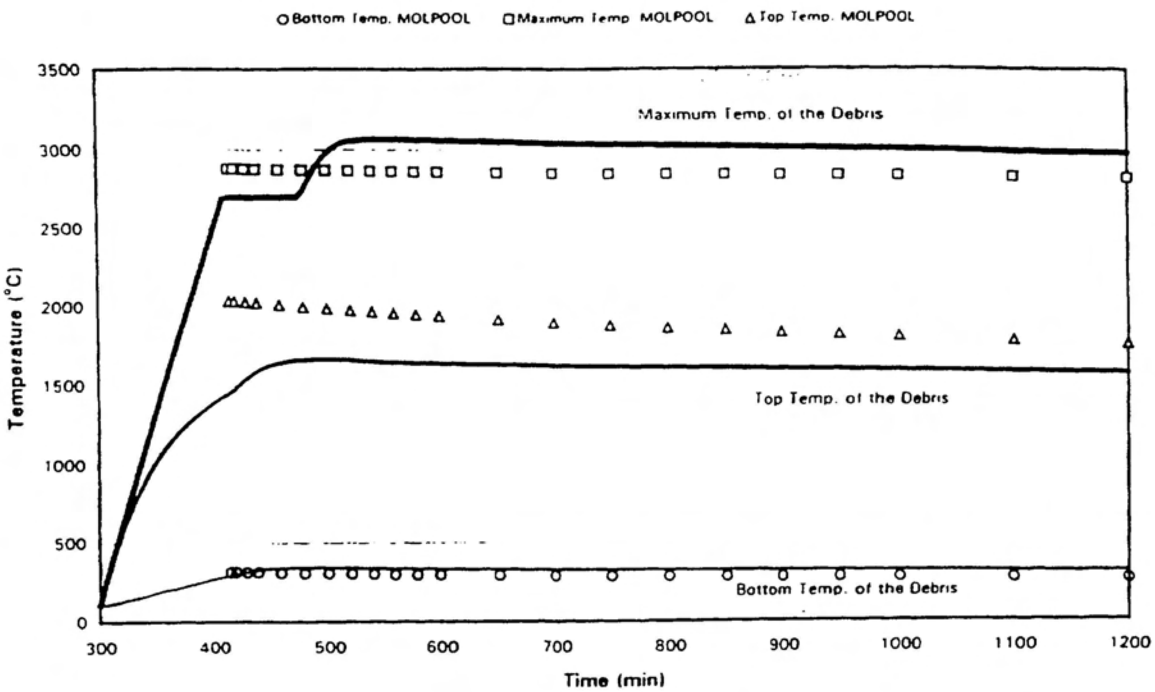

Figure 2: Comparison of Selected Temperatures Predicted by DEBRIS.MLT and MOLPOOL. Reference Conditions.

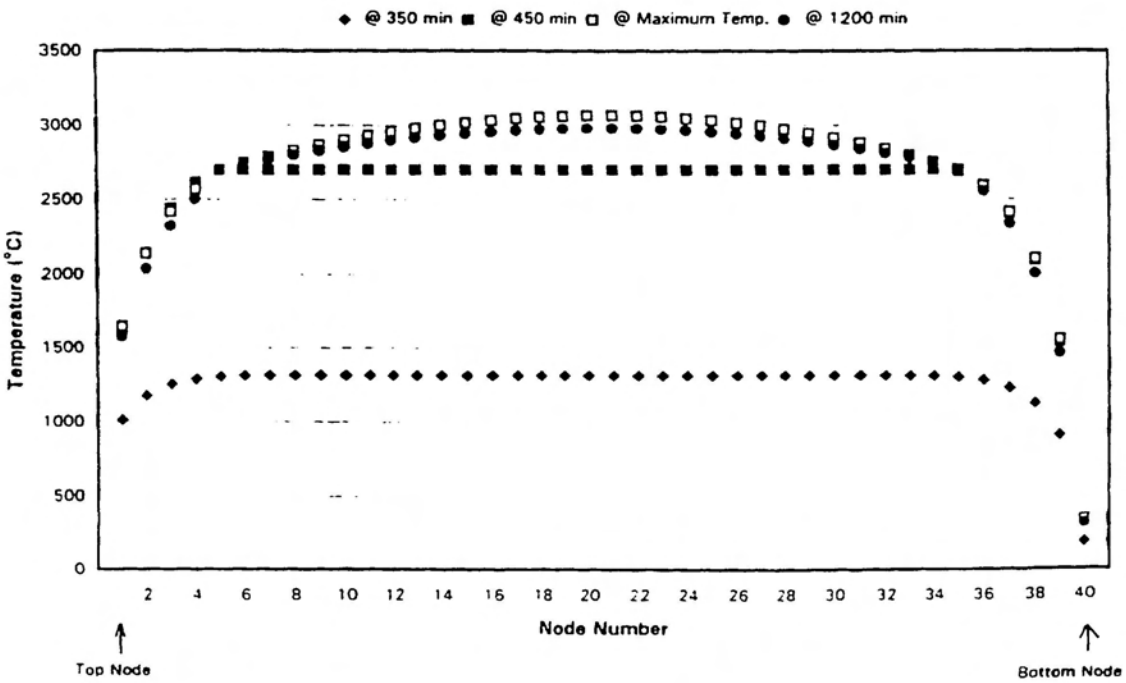

Figure 3: Temperature Profiles Through The Corium at Different Times. Reference Conditions.

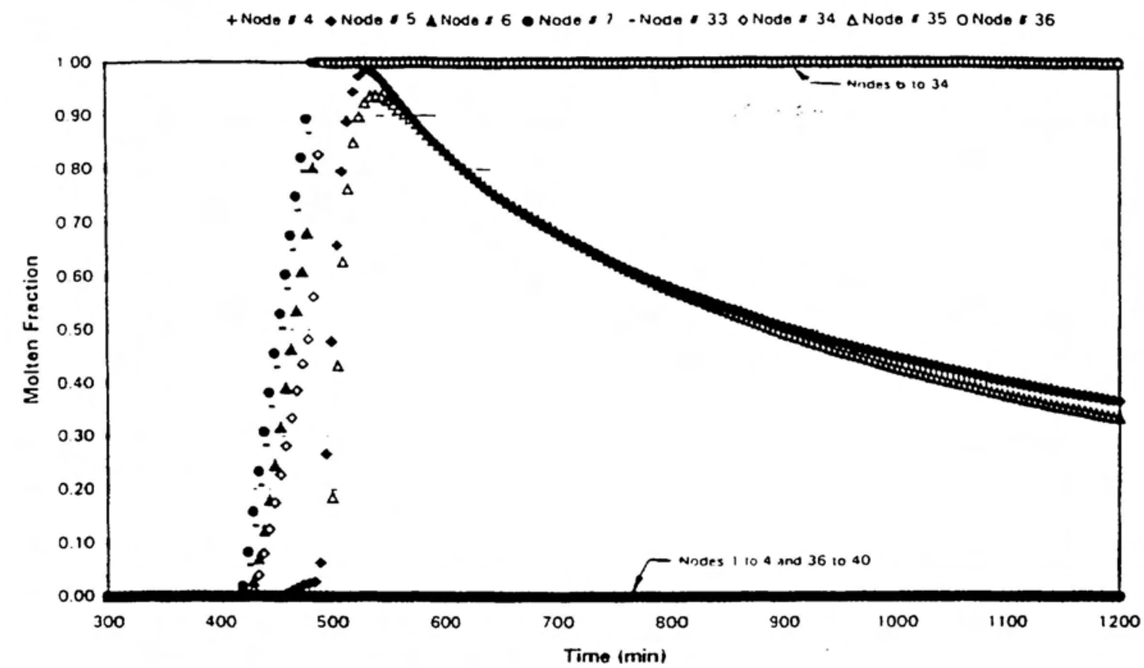

Figure 4: Molten Fraction at Different Positions. Reference Conditions.

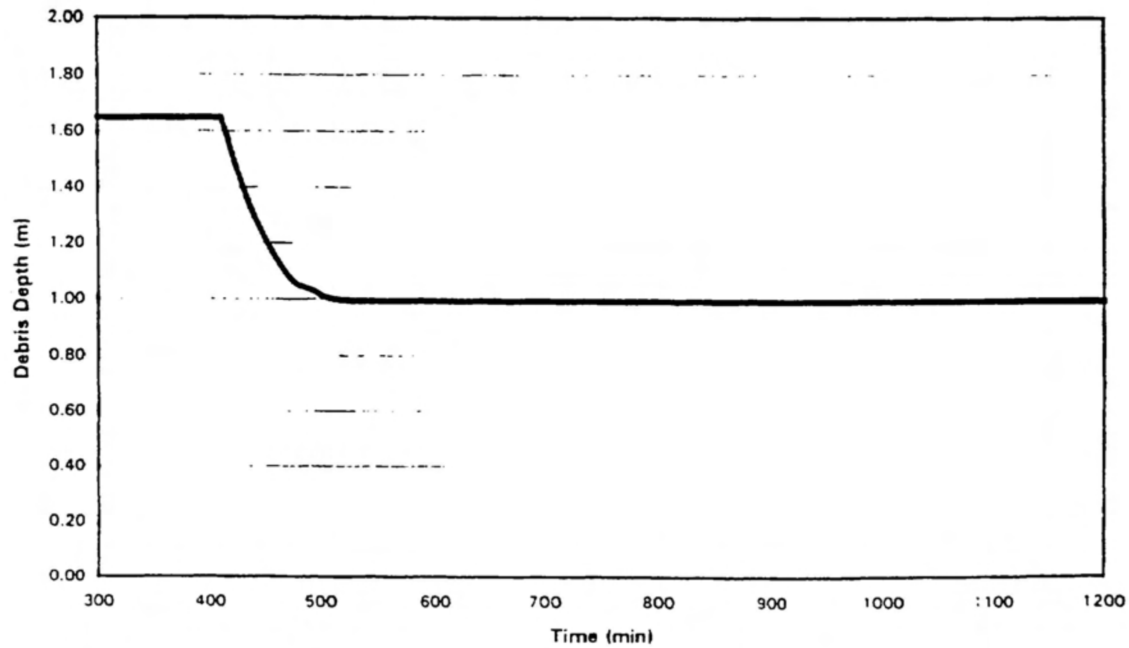

Figure 5: Debris Depth in Debris Melting Transient. Reference Conditions.

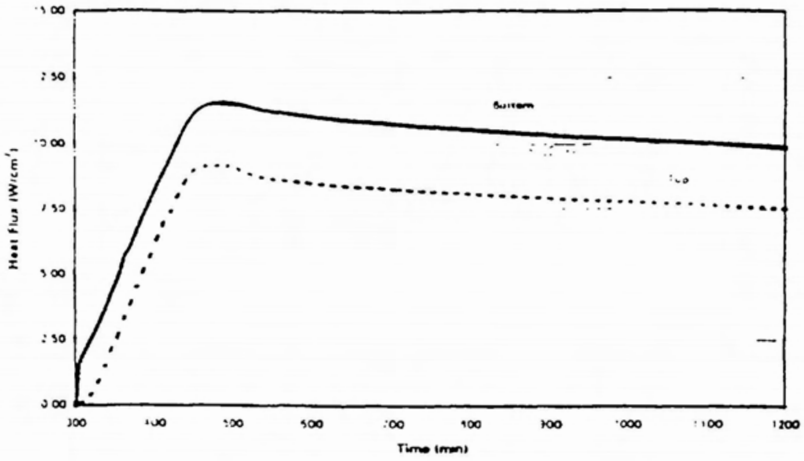

Figure 6: Heat Fluxes on Calandria Wall in Debris Melting Transient. Reference Conditions.

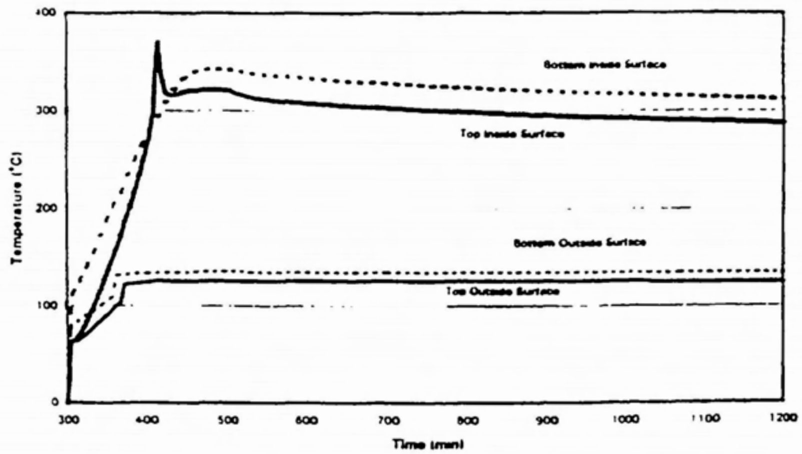

Figure 7: Calandria Wall Temperatures in Debris Melting Transient. Reference Conditions.

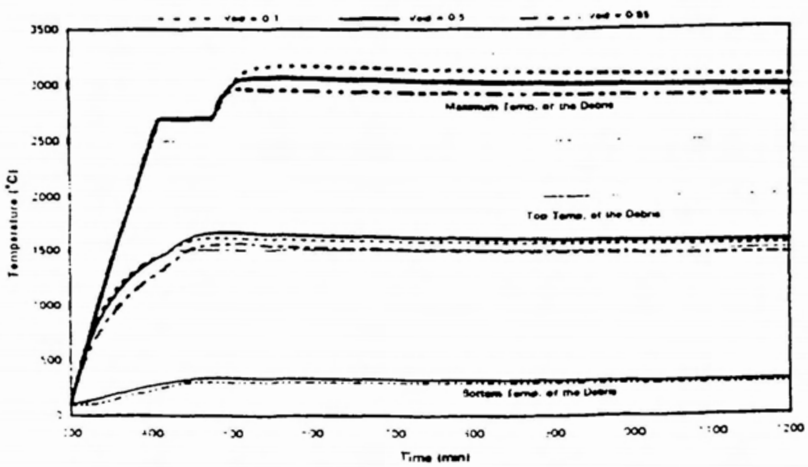

Figure 8: Effects of Porisity on Debris Temperatures. Pore Size = 3 cm.